

CHEMICAL PHYSICS
OF BIOLOGICAL PROCESSES

**Kinetics, Equilibrium and Thermodynamic Investigation
of New Coccine Adsorption onto Chitosan 10B in Aqueous Solution**

M. Islam^a, P. Ghosh^a, S. Karmaker^a, and T. K. Saha^{a, *}

^a Department of Chemistry, Jahangirnagar University, Savar, Dhaka, 1342 Bangladesh

*e-mail: tksaha_ju@yahoo.com

Received May 14, 2021; revised September 28, 2021; accepted October 20, 2021

Abstract—Adsorption characteristics of new coccine on chitosan 10B were examined in aqueous medium. The zero point charge (pH_{zpc}) of chitosan 10B was evaluated to be 6.45. In order to find out an optimum condition for maximum dye elimination by chitosan 10B, the kinetic investigations were carried out as a function of contact time, solution pH, initial dye concentration, temperatures, and ionic strengths, respectively. The maximum dye removal by chitosan 10B was found in acidic medium at pH 4. The kinetics of dye adsorption data was analyzed by pseudo first-order, pseudo second-order, Elovich, film diffusion and intraparticle diffusion kinetic models, respectively. The kinetic data complied with pseudo second-order kinetic model. Adsorption isotherms were agreed perfectly with Langmuir isotherm model having maximum dye adsorption ability $90.77 \mu\text{mol/g}$ at 30°C . New coccine adsorption onto chitosan 10B was proven by the Fourier Transform Infrared (FTIR) spectroscopy. Thermodynamic parameters indicate that the new coccine dye elimination from aqueous solution by chitosan 10B is an exothermic spontaneous physisorption process. New coccine desorption from dye-loaded chitosan 10B was performed in 0.1 mol/L NaOH solution (pH 13) and the reusability of chitosan 10B was also investigated.

Keywords: new coccine, chitosan 10B, adsorption, kinetics, thermodynamics

DOI: 10.1134/S1990793121100043

INTRODUCTION

Now-a-days the discharge of azo dyes into the nature is a big trouble for the pigmentation of the native waters, their toxicity, carcinogenicity, mutagenicity, and also their biotransformation products [1]. The colored wastewater imposes serious health problems for both aquatic and human lives. The dyed wastewater also interrupts aesthetics, water clarity, and gas solubility in water environments [2]. Moreover, there is a typical concern that the azo dyes diminish the permeation of light into water and there by disturbing the photosynthetic activity of aquatic floras [3]. So, it is very urgent to eliminate azo dyes from wastewater.

Various techniques such as oxidative degradation [4], photocatalytic degradation [5–7] coagulation [8], flocculation [9], membrane filtration [10], adsorption [11–14], ozonation [15], liquid-liquid extraction [16], and biological process [17] are used to remove dyes from wastewater. Each method presents some drawbacks. The major drawbacks are cost, efficiency, selectivity to toxic elements, availability etc. Among the mentioned processes, adsorption is one of the best methods due to its small expense, ease mode of operation and finally in selectivity to toxic materials. Various adsorbents such as activated carbon [18], graphene

[19], clay [20], silica [21], fly ash [22], peat [23] and agro wastes [24–26] etc. have been utilized to eliminate the dyes from aqueous solution.

On other hand, chitosan is a linear polysaccharide made in arbitrarily scattered β -(1 → 4)-coupled D-glucosamine (deacetylated unit) and N-acetyl-D-glucosamine (acetylated unit). Chitosan is synthesized by treating chitin with sodium hydroxide. Chitin is usually obtained from garbage of the seafood handling industries, commonly shells of krill, shrimp, crabs, and prawns. Shrimp shell rubbish is a bulky garbage of seafood handling industries in Bangladesh (more than 30000 tons per year) [12]. The large numbers of amino and hydroxyl functional groups in chitosan assemble it valuable for eliminating various dyes from aqueous systems. Recently, we have investigated the adsorption behaviors of remazol brilliant violet, reactive blue 4 (RB4), reactive yellow 145 (RY145), and reactive red 239 (RR239), and onto chitosan in aqueous media [11, 12, 27, 28]. Chitosan showed intense dye adsorption pursuit. This significant discovery inspired us to examine adsorption features of new coccine dye (Fig. 1a) onto chitosan in aqueous medium.

In this paper, chitosan 10B (100% deacetylated chitin, Fig. 1b) was utilized as an adsorbent to eliminate an azo dye new coccine from aqueous system. The influences of contact time, solution pH, dye con-

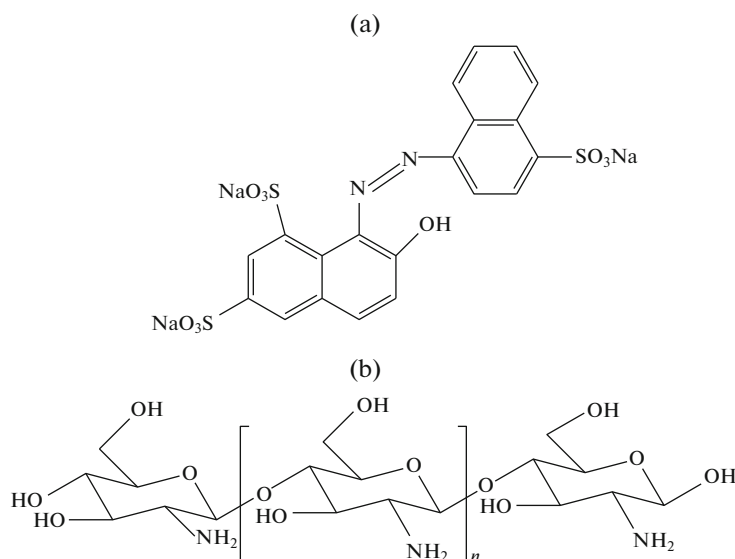


Fig. 1. The structures of new coccine (a) and chitosan 10B (b).

centration, temperatures and ionic strengths on the kinetics of new coccine adsorption onto chitosan 10B were examined in aqueous medium through batch adsorption studies. The equilibrium adsorption of new coccine onto chitosan 10B was explored at four different temperatures. Dye adsorption kinetics and mechanisms were inspected by pseudo first-, second-order, Elovich, film, and intraparticle diffusion models. Freundlich, Langmuir and Temkin isotherm models were applied to assess new coccine dye adsorption equilibrium. Thermodynamics of the sorption phenomena and reusability of recycled chitosan 10B were also investigated.

EXPERIMENTAL

Materials

New coccine (C₂₀H₁₁N₂Na₃O₁₀S₃; MW: 604.47; dye content 75%; Fig. 1a) dye was bought from Sigma-Aldrich, Germany and was used without any sanitization. Chitosan 10B (Fig. 1b) was bought from Katokichi Bio Co., Ltd., Japan and employed as received. Other chemicals employed in this research were of pure analytical grade. Water used in all experiments was distilled and deionized.

Characterization of Chitosan 10B

The mass median diameter of the chitosan 10B particles was estimated to be (228 ± 5) μm by a laser scattering particle size analyzer (LDSA-240DA, Tonichi Computer Applications, Japan) coupled with a dry dispersing apparatus (PD-10S, Tonichi Computer Applications, Japan). The point of zero charge (pH_{zpc}) of chitosan 10B was determined by pH drift method [29]. A solution of 0.1 mol/L KCl solution was

prepared and boiled to remove dissolved CO₂ and then cooled to room temperature. The initial pH of KCl solution was adjusted between 2.0 and 12.0 by using 0.5 mol/L HCl or 0.5 mol/L NaOH. Chitosan 10B (0.05 g) was added into 25 mL of the pH-adjusted 0.1 mol/L KCl in a 125 mL reagent bottle. The bottles containing chitosan 10B samples were kept closed and equilibrated for 24 h. After 24 h, the final pH of each sample was measured and plotted against the initial pH. The pH at which the curve crosses the pH_{initial} = pH_{final} line is taken as pH_{pzc} of chitosan 10B. Fourier transformation infrared (FTIR) spectra of chitosan 10B and dye-loaded chitosan 10B were recorded in KBr at the frequency range 400–4000 cm⁻¹ by using FTIR spectrometer (IRPrestige-21 FTIR Spectrophotometer, Shimadzu, Japan).

Adsorption Study

To evaluate the features of new coccine dye adsorption onto chitosan 10B, group adsorption tests were executed in stoppered bottle (125 mL) having chitosan 10B (0.05 g) and dye solution (25 mL; 50 μmol/L) [11]. The primary pH of dye solution was corrected with 1 mol/L HCl or NaOH solution, by employing a pH meter (Adwa AD8000). Sample bottles were agitated in a thermostated shaker at room temperature (30 ± 0.2°C) with 120 rpm until equilibrium. Every bottle was plugged to prevent vaporization at higher temperature. Sample bottles were taken at definite time period for computing dye concentration in solution. The samples were centrifuged at 4000 rpm for 5 min. New coccine concentration in the supernatant was computed by the spectrophotometric method, employing a Shimadzu UV-1800 spectrophotometer (Shimadzu, Japan), at λ_{max}: 507 nm (pH 1–10) and

438 nm (pH 11–13). The apparent molar absorptivity constants of new coccine were determined to be $18 \times 10^3 \text{ L mol}^{-1} \text{ cm}^{-1}$ at 507 nm and $9 \times 10^3 \text{ L mol}^{-1} \text{ cm}^{-1}$ at 438 nm. The amount of new coccine adsorbed per unit mass of chitosan 10B at time t , q_t ($\mu\text{mol/g}$) was computed by Eq. (1)

$$q_t = \frac{V(C_0 - C_t)}{m}, \quad (1)$$

where C_0 ($\mu\text{mol/L}$) and C_t ($\mu\text{mol/L}$) are new coccine strengths in solution at zero and at time t , respectively; V (L) is the volume of new coccine solution and m (g) is the quantity of dry chitosan 10B utilized.

The adsorption kinetics was also examined at different solution pHs (4–10), dye concentration (100–2000 $\mu\text{mol/L}$), temperatures (30, 35, 40 and 45°C), and ionic strengths (0.01–0.05 mol/L), respectively. The ionic strength of dye solution was controlled with 1 mol/L KCl solution. Adsorption equilibrium was executed in aqueous medium (pH 4) at various temperatures (30, 35, 40 and 45°C) in absence KCl. The extent of new coccine adsorbed onto adsorbent at equilibrium time, q_e ($\mu\text{mol/g}$) was computed by Eq. (2)

$$q_e = \frac{V(C_0 - C_e)}{m}, \quad (2)$$

where C_e ($\mu\text{mol/L}$) is the new coccine strength in solution at equilibrium time; C_0 , V and m persist analogous as illustrated earlier.

In desorption experiment, chitosan 10B was treated with new coccine solution (50 $\mu\text{mol/L}$; 25 mL) for 120 min, separated and dye loaded-chitosan 10B was dehydrated at room temperature (30°C) for 12 h. New coccine filled-chitosan 10B particles were shaken in 0.1 mol/L NaOH solution (25 mL; pH 13) for 120 min. The extent of dye adsorption was ascertained in the similar way as mentioned previously. All data reported in this article are the average of dual measurements.

RESULTS AND DISCUSSION

Interaction Time Effect

The influence of interaction time on new coccine adsorption kinetics was observed in aqueous medium (pH 4) at 30°C. The effects are exhibited in Fig. 2. The typical time-resolved UV–visible spectra of new coccine during adsorption onto chitosan 10B are shown in Fig. 2a. It is noted that the absorbance of new coccine at 507 nm was gradually diminished with rising contact time. These effects signify that the magnitude of new coccine removal by chitosan 10B was gradually amplified with rising contact time. The influence of interaction time on the degree of new coccine adsorption (q_t) onto adsorbent is exhibited in Fig. 2b. It is perceived that the degree of new coccine adsorption was very rapid for first 20 min, later the dye adsorption rate diminished slowly and accomplished to equilib-

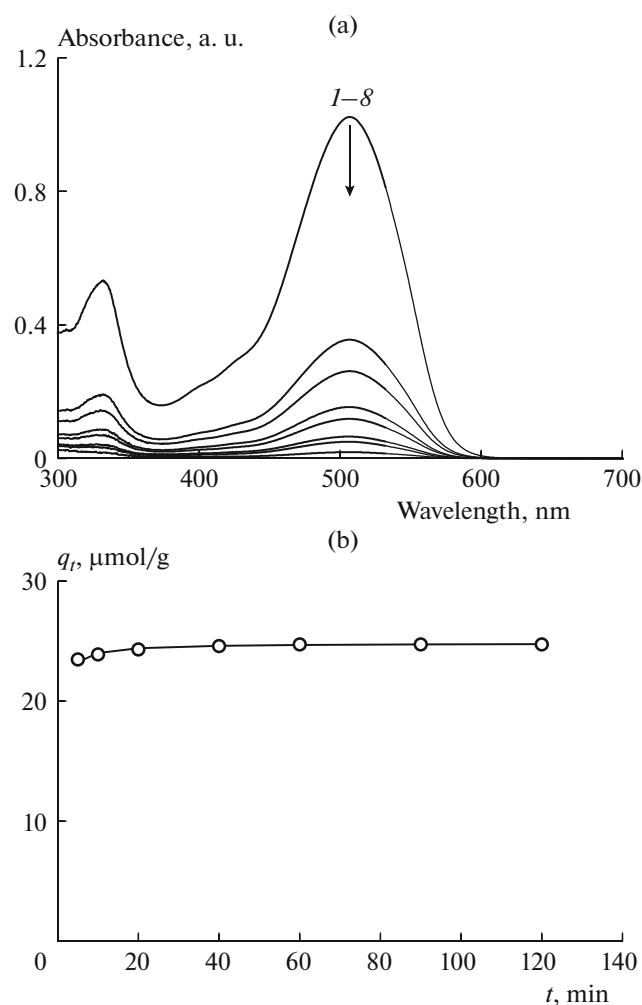


Fig. 2. (a) Typical UV–visible spectra of new coccine taken at 1–0, 2–5, 3–10, 4–20, 5–40, 6–60, 7–90, and 8–120 min during adsorption onto chitosan 10B in aqueous medium (pH = 4) at 30°C. (b) The extent of new coccine adsorption, q_t ($\mu\text{mol/g}$) onto chitosan 10B with contact time, t (min). [New coccine] $_0$: 50 $\mu\text{mol/L}$; solution volume—25 mL; adsorbent dosage—0.05 g; solution pH 4; temperature—30°C.

rium within 60 min. At the starting, the rate of dye adsorption was fast as the dye molecules were adsorbed by the peripheral surface of chitosan 10B. When the surface adsorption attained to saturate, the dye molecules slowly penetrate into the holes of the adsorbent particles [30]. However, the extent of adsorption was measured for 120 min as an optimum equilibrium time for further studies.

Effect of Solution pH

The exterior charges of adsorbent and the structure of dye molecules are greatly influenced by solution pH [31]. Hence, the solution pH plays a major role on the dye elimination process. Here, the adsorption of new

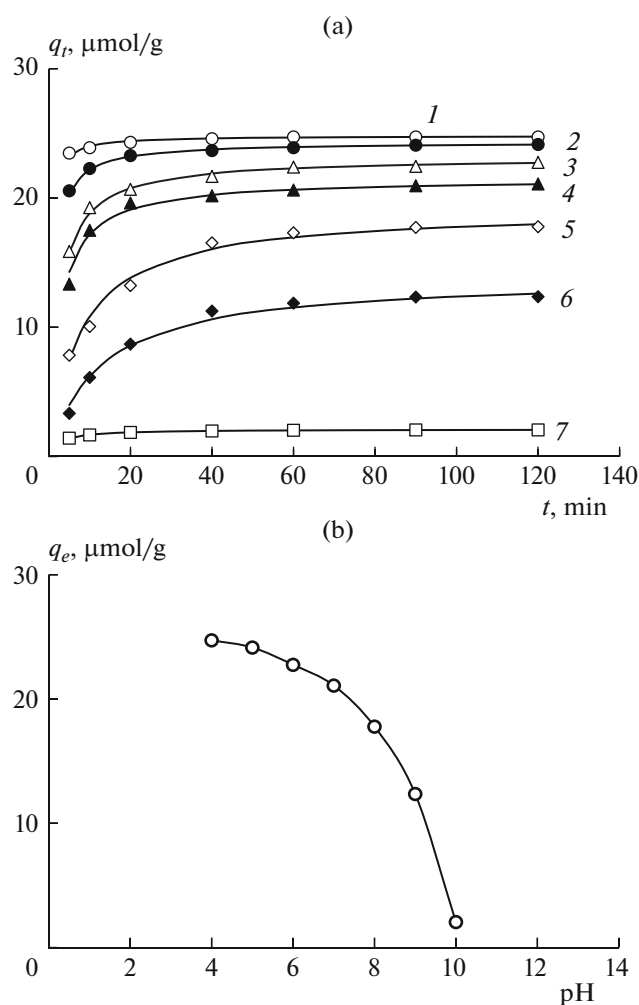


Fig. 3. (a) The changes in extent of new coccine adsorption, q_t ($\mu\text{mol/g}$), onto chitosan 10B with contact time, t (min), at various solution pHs. [New coccine] $_0$: 50 $\mu\text{mol/L}$, solution volume—25 mL, adsorbent dosage—0.05 g, temperature—30°C, solution pHs: 1—pH 4, 2—pH 5, 3—pH 6, 4—pH 7, 5—pH 8, 6—pH 9, 7—pH 10. All lines were numerically mimicked by utilizing Eq. (4), $q_{e(\text{cal})}$ and k_2 recorded in Table 1. (b) The extent of equilibrium new coccine adsorption, q_e ($\mu\text{mol/g}$), onto chitosan 10B at several solution pHs.

coccine onto chitosan 10B was performed in aqueous media at pH 4–10 with a fixed dye concentration (50 $\mu\text{mol/L}$) and chitosan 10B (0.05 g) for 120 min. Adsorption research was not performed at very low pH due to the solubility of chitosan 10B [13]. New coccine dye adsorption kinetic sketches at numerous solution pHs are shown in Fig. 3a. Initial dye elimination rate, h ($\mu\text{mol/g min}$), fallen considerably with rising solution pHs (Table 1). From Fig. 3b, it is said that the equilibrium dye adsorption quantity, q_e ($\mu\text{mol/g}$), also decreased with rising solution pHs. These results can be explained with the help of pH_{zpc} of chitosan 10B. The pH_{zpc} of chitosan 10B was found to be 6.45 (figure not shown), which is consistent with the reported

pH_{zpc} : 6.3 of chitosan [32]. At pH 4, the surface of chitosan 10B became positively charged which attracted the anionic dye molecules, hence the new coccine adsorption rate and adsorption quantity became high at this solution pH. On the contrary, with rising the solution $\text{pH} > \text{pH}_{\text{zpc}}$, the surface of chitosan 10B particles converted into negative charges resulting electrostatic repulsion between chitosan 10B and new coccine dye molecules [13], which ultimately results in less adsorption of dye. The highest quantity of new coccine dye adsorption onto chitosan 10B was obtained to be 24.72 $\mu\text{mol/g}$ in aqueous solution (pH 4). A comparable result was also noticed in RB4 anionic dye adsorption onto chitosan 10B [12]. Hence, all other kinetic experiments were conducted at solution pH 4.

Dye Concentration Effect

The extent of new coccine adsorption (q_t) onto chitosan 10B with contact time (t) at various initial concentration of dye solutions (pH 4) and at 30°C is illustrated in Fig. 4. The initial dye elimination rate, h ($\mu\text{mol/g min}$), increased with rising dye concentration in solution (Table 1), which indicates that the new coccine elimination by chitosan 10B definitely depends on its concentration in solution. The values of q_e were noticed to be 24.72 $\mu\text{mol/g}$ for 50 $\mu\text{mol/L}$ and 94.12 $\mu\text{mol/g}$ for 2000 $\mu\text{mol/L}$ new coccine dye solutions, respectively. The dye concentration in solution affords a prominent potency to devastate the mass transfer confrontation of all molecules between the liquid and solid phases [11]. A comparable phenomenon was also seen in the elimination of remazol brilliant violet by chitosan 10B and reactive orange (RO13) by jackfruit seed flakes in aqueous medium [11, 26].

Ionic Strength Effect

The changes in degree of new coccine adsorption (q_t) onto chitosan 10B with contact time (t) in aqueous medium (pH 4) was examined at numerous ionic strengths using known amount of KCl in dye solution (50 $\mu\text{mol/L}$) at 30°C. The effects are depicted in Fig. 5. It is found that the capacity of equilibrium dye adsorption, q_e ($\mu\text{mol/g}$), onto chitosan 10B gradually decreased with rising ionic strength of dye solutions. The results could be explained by a competitive effect between new coccine dye anions and Cl^- (from KCl) for the active sorption sites of chitosan 10B as noticed in elimination of RO13 by jackfruit seed flakes [26] and RY145 by chitosan in aqueous media [27], respectively. This also demonstrates the presence of electrostatic interactions between dye molecules and adsorbent particles.

Table 1. Kinetic parameters noticed from different kinetic models employed to new coccine adsorption onto chitosan 10B in aqueous media

Parameters	Pseudo first-order kinetics				Pseudo second-order kinetics				Elovich kinetics						
	$q_{e(\text{exp})}$, $\mu\text{mol/g}$	$q_{e(\text{cal})}$, $\mu\text{mol/g}$	k_1 , min^{-1}	R^2	Δq_t , %	$q_{e(\text{cal})}$, $\mu\text{mol/g}$	k_2 , ($\text{g}/\mu\text{mol}$) min	h , ($\mu\text{mol/g}$) min	R^2	Δq_t , %	$q_{e(\text{cal})}$, $\mu\text{mol/g}$	α , ($\mu\text{mol/g}$) min	β , $\text{g}/\mu\text{mol}$	R^2	Δq_t , %
Solution pH 4–10; [Dye] ₀ : 50 $\mu\text{mol/L}$, temperature 30°C															
4	24.72	1.58	0.06	0.994	6.49	24.81	12.00×10^{-02}	74.07	1.000	0.40	24.89	1.71×10^{24}	2.47	0.932	0.56
5	24.14	3.09	0.05	0.971	6.34	24.33	4.00×10^{-02}	25.19	0.999	0.60	24.54	1.48×10^{08}	0.96	0.883	0.87
6	22.75	5.24	0.04	0.911	6.13	23.15	2.00×10^{-02}	10.02	0.999	0.93	23.46	2.07×10^{03}	0.50	0.899	1.23
7	21.08	5.73	0.04	0.946	6.20	21.51	2.00×10^{-02}	8.51	0.999	1.04	21.98	4.45×10^{02}	0.46	0.839	1.50
8	17.78	14.47	0.06	0.997	3.41	19.12	1.00×10^{-02}	2.49	0.999	2.17	18.84	7.46×10^{00}	0.30	0.959	1.74
9	12.36	13.69	0.05	0.978	3.11	13.91	1.00×10^{-02}	1.12	0.997	3.35	13.42	2.35×10^{00}	0.34	0.955	2.78
10	2.06	0.70	0.05	0.988	18.87	2.10	19.00×10^{-02}	0.84	1.000	3.24	2.14	7.81×10^{01}	5.04	0.927	4.45
[Dye] ₀ : 100–2000 ($\mu\text{mol/L}$); solution pH 4; temperature 30°C															
100	37.36	18.16	0.06	0.994	3.91	38.61	7.00×10^{-03}	10.58	0.999	1.00	38.59	2.59×10^{02}	0.23	0.963	0.99
250	69.44	41.15	0.05	0.982	2.55	73.53	2.00×10^{-03}	11.27	0.999	0.97	74.99	4.20×10^{01}	0.08	0.948	1.13
500	87.50	48.00	0.05	0.980	2.39	91.74	2.00×10^{-03}	17.61	0.999	0.78	94.23	8.72×10^{01}	0.07	0.932	0.99
1000	90.01	47.91	0.05	0.979	2.40	94.34	2.00×10^{-03}	18.90	0.999	0.77	96.61	1.03×10^{02}	0.07	0.932	0.95
1500	93.25	11.05	0.05	0.997	3.24	97.09	2.00×10^{-03}	20.70	0.999	0.70	99.94	1.30×10^{02}	0.07	0.932	0.92
2000	94.12	48.00	0.05	0.980	2.41	98.04	2.00×10^{-03}	21.19	0.999	0.70	100.79	1.38×10^{02}	0.07	0.932	0.91
Ionic strength: 0.01–0.05 (mol/L); solution pH 4; [Dye] ₀ : 50 $\mu\text{mol/L}$; temperature 30°C															
0.01	21.08	1.79	0.04	0.968	6.95	21.19	6.90×10^{-02}	31.15	1.000	0.52	21.30	4.95×10^{12}	1.62	0.929	0.74
0.02	17.23	1.75	0.04	0.962	7.61	17.33	7.00×10^{-02}	20.88	1.000	0.61	17.45	5.92×10^{09}	1.59	0.891	0.92
0.03	14.22	2.11	0.05	0.995	8.16	14.35	6.60×10^{-02}	13.61	1.000	0.85	14.44	8.54×10^{07}	1.63	0.946	1.10
0.05	11.61	2.68	0.04	0.995	8.58	11.79	4.40×10^{-02}	6.10	0.999	1.22	11.81	4.14×10^{04}	1.33	0.978	1.28
Temperature: 35–45 (°C); solution pH 4; [Dye] ₀ : 50 $\mu\text{mol/L}$															
35	23.56	2.11	0.04	0.994	6.55	23.70	5.90×10^{-02}	33.33	1.000	0.53	23.73	1.02×10^{14}	1.58	0.969	0.59
40	21.97	3.95	0.05	0.997	6.44	22.22	3.40×10^{-02}	16.69	1.000	0.76	22.33	4.96×10^{06}	0.90	0.963	0.91
45	20.89	3.97	0.04	0.983	6.56	21.14	2.90×10^{-02}	13.11	1.000	0.80	21.33	1.47×10^{05}	0.77	0.937	1.06

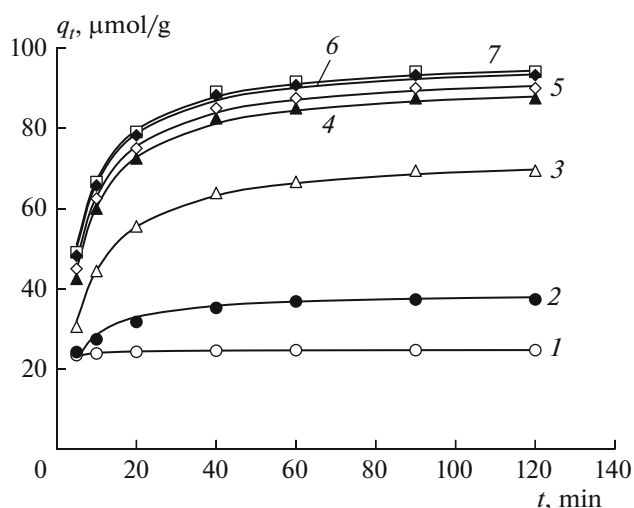


Fig. 4. The changes in extent of new coccine dye elimination, q_t ($\mu\text{mol/g}$), by chitosan 10B with contact time (t) at various initial concentration of dye solution. Solution pH 4, solution volume—25 mL, adsorbent dosage: 0.05 g, temperature: 30°C, [New coccine] $_0$: 1—50, 2—100, 3—250, 4—500, 5—1000, 6—1500, 7—2000 $\mu\text{mol/L}$. All lines were numerically mimicked by utilizing Eq. (4), $q_{e(\text{cal})}$ and k_2 (Table 1).

Temperature Effect

New coccine adsorption kinetics was explored in aqueous medium (pH 4) at various temperatures (30, 35, 40 and 45°C) with dye solution (50 $\mu\text{mol/L}$; 25 mL) for 120 min. The effects are exhibited in Fig. 6. The dye elimination rate, h ($\mu\text{mol/g min}$), and the degree of adsorption at equilibrium, q_e ($\mu\text{mol/g}$), declined with rising solution temperature from 30 to 45°C (Table 1). The interaction between new coccine dye molecules and functional groups of chitosan 10B occurred less efficiently at higher temperature due to inadequate flexibility of the dye molecules at higher temperature. It is foreseen that the high solution temperature may compress the surface area and the interior configuration of chitosan 10B as observed in adsorption of brilliant green onto kaolin [33], methylene blue and indigo carmine onto Brazil nut shells [34] in aqueous solution.

Kinetic Modeling

To describe the mechanism of new coccine dye adsorption onto chitosan 10B, the data procured from batch adsorption explorations were studied by pseudo first- [35], second-order [36], Elovich [37], film diffusion [38], and intraparticle diffusion [39] kinetic models, respectively. The pseudo first-order kinetic model is known by Eq. (3) [35]:

$$\log(q_e - q_t) = \log q_e - \frac{k_1}{2.0303} t, \quad (3)$$

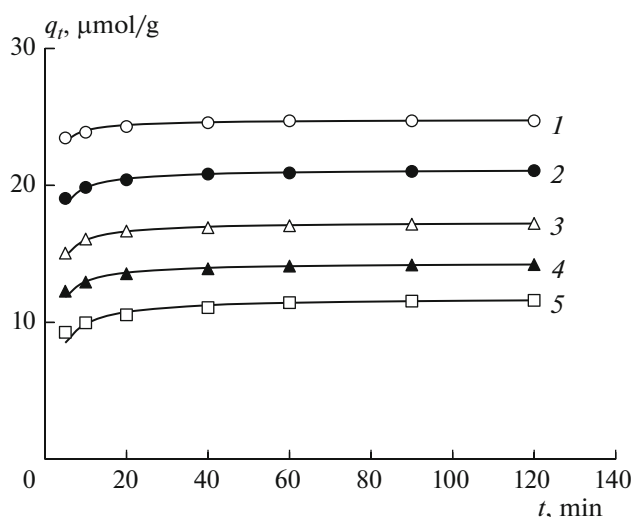


Fig. 5. The changes in extent of new coccine adsorption, q_t ($\mu\text{mol/g}$), onto chitosan 10B with contact time, t (min), at various ionic strengths of dye solution. Solution pH 4, [New coccine] $_0$: 50 $\mu\text{mol/L}$, solution volume—25 mL, adsorbent dosage—0.05 g, temperature—30°C, ionic strength: 1—0.00, 2—0.01, 3—0.02, 4—0.03, 5—0.05 mol/L. All lines were numerically simulated by utilizing Eq. (4), $q_{e(\text{cal})}$ and k_2 (Table 1).

where k_1 (min^{-1}) is the pseudo first-order sorption rate constant determined from the slope of a plot $\log(q_e - q_t)$ versus t .

The nonlinear form pseudo second-order kinetic model is stated by Eq. (4) [36]:

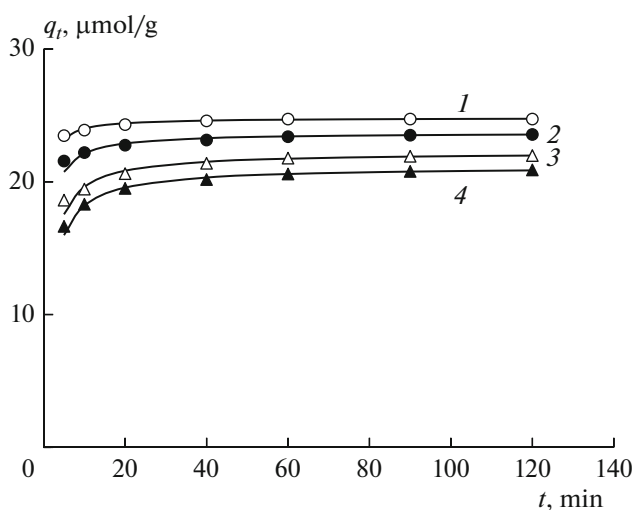


Fig. 6. The changes in extent of new coccine dye adsorption (q_t) onto chitosan 10B with contact time (t) in aqueous medium at different temperatures. Solution pH 4, [New coccine] $_0$: 50 $\mu\text{mol/L}$, solution volume—25 mL, adsorbent dosage: 0.05 g, temperature—1—30, 2—35, 3—40, 4—45°C. All lines were numerically simulated by employing Eq. (4), $q_{e(\text{cal})}$ and k_2 (Table 1).

$$q_t = \frac{k_2 q_e^2 t}{(1 + k_2 q_e t)}, \quad (4)$$

where k_2 ((g/ μ mol) min) is a pseudo second-order adsorption rate constant obtained from Eq. (5) [36]:

$$\frac{t}{q_t} = \frac{1}{k_2 q_e^2} + \frac{1}{q_e} t. \quad (5)$$

The k_2 and q_e values were computed from intercept and slope of a plot t/q_t versus t . The initial elimination rate, h ((μ mol/g) min), is calculated by Eq. (6) [36]:

$$h = k_2 q_e^2. \quad (6)$$

Elovich kinetic model is stated by Eq. (7) [37]:

$$q_t = \frac{1}{\beta} \ln(\alpha\beta) + \frac{1}{\beta} \ln t, \quad (7)$$

where α ((μ mol/g) min) denotes a primary dye adsorption rate and β (g/ μ mol) is involved to an activation energy of chemisorption and an extent of surface coverage. The Elovich constants were obtained from q_t versus $\ln t$ plot.

The significance and validity of each model can be verified using a normalized standard deviation (Δq_e %) [40], which can be determined as follows:

$$\Delta q_e (\%) = 100 \sqrt{\frac{\sum [(q_{e, \text{exp}} - q_{e, \text{cal}}) / q_{e, \text{exp}}]^2}{N - 1}}, \quad (8)$$

where N is the quantity of data points, $q_{e, \text{exp}}$ (μ mol/g) and $q_{e, \text{cal}}$ (μ mol/g) are the quantity of experimental and calculated equilibrium dye adsorption.

The kinetic parameters along with correlation coefficients (R^2) and normalized standard deviation (Δq_e %) found in different kinetic models are shown in Table 1. The R^2 values attained from pseudo first-order (≤ 0.997) and Elovich (≤ 0.969) kinetic models were negligible compare to the values computed from pseudo second-order (≥ 0.999) kinetic model (Table 1). And the values of Δq_e (%) attained from pseudo second-order kinetic model were small compare to the values found in pseudo first-order and Elovich kinetic models (Table 1). In addition, the $q_{e, \text{cal}}$ values computed from pseudo second-order kinetic model and the observed $q_{e, \text{exp}}$ values are analogous (Table 1) implying a good agreement of pseudo second-order adsorption kinetics as found in RY145 and reactive black 5 (RB5) adsorption on chitosan in aqueous media [27, 38].

The equation of film diffusion model proposed by McKay can be written as [38]:

$$\ln(1 - F) = -k_{fd} t, \quad (9)$$

$$F = \frac{q_t}{q_\infty}, \quad (10)$$

where k_{fd} (1/min) is a film diffusion rate constant, F is a partial equilibrium achievement, and q_t (μ mol/g)

and q_∞ (μ mol/g) are extents of new coccine adsorption onto chitosan 10B at t time and infinite time, respectively. The film diffusion rate constant was determined from the plot of $\ln(1 - F)$ versus t . The values of k_{fd} and R^2 are shown in Table 2.

The intraparticle diffusion model is denoted by Eq. (11) [39]:

$$q_t = k_{id} t^{0.5} + I, \quad (11)$$

where k_{id} ((μ mol/g) min^{0.5}) represents intraparticle diffusion rate constant and I (μ mol/g) signifies the intercept. Figure 7 shows the usual plots of q_t versus $t^{0.5}$ of new coccine dye adsorption onto chitosan 10B at different dye concentrations in solution. There were two linear portions in each plot, which suggests that two phenomena occurred in the adsorption process. The first is prompt exterior surface diffusion of the adsorbent with a rate constant k_{id1} ((μ mol/g) min^{0.5}) and the second is slow interior surface diffusion of the adsorbent with a rate constant k_{id2} ((μ mol/g) min^{0.5}) [27]. The k_{id1} ((μ mol/g) min^{0.5}) and k_{id2} ((μ mol/g) min^{0.5}) values presented in Table 2 were determined from the slope of corresponding lines in Fig. 7. Any straight line did not pass across the origin (Fig. 7) indicating the mechanism of present dye adsorption is multifaceted. Surface adsorption and intraparticle diffusion mechanisms might be responsible to the actual sorption process as noticed in the RY145 adsorption onto chitosan in aqueous medium [27].

Adsorption Isotherm

The extent of equilibrium new coccine elimination by chitosan 10B was examined in aqueous system at numerous temperatures. The plots of q_e (μ mol/g) versus C_e (μ mol/L) at numerous solution temperatures are depicted in Fig. 8. The present adsorption was found to be an exothermic process as the magnitude of q_e (μ mol/g) decreased with rising solution temperature from 30 to 45°C. Freundlich [41], Temkin [42], and Langmuir [43] isotherm models were employed to elucidate equilibrium adsorption data acquired at various temperatures. Equations of the employed isotherm models are given below:

Freundlich model:

$$\text{nonlinear form } q_e = K_F C_e^{\frac{1}{n}}, \quad (12)$$

$$\text{linear form } \ln q_e = \frac{1}{n} \ln C_e + \ln K_F, \quad (13)$$

Temkin model:

$$\text{nonlinear form } q_e = \frac{RT}{b} \ln(K_T C_e), \quad (14)$$

$$\text{linear form } q_e = \frac{RT}{b} \ln K_T + \frac{RT}{b} \ln C_e. \quad (15)$$

Table 2. Values of diffusion rate constants for the new coccine dye adsorption onto chitosan 10B

Parameters	Film diffusion model		Intra-particle diffusion model			
	k_{fd} , min ⁻¹	R^2	k_{id1} , (μmol/g) min ^{0.5}	R^2	k_{id2} , (μmol/g) min ^{0.5}	R^2
Solution pH 4–10; [Dye] ₀ : 50 μmol/L, temperature 30°C						
4	0.06	0.994	0.37	0.990	0.03	0.578
5	0.05	0.971	1.18	0.938	0.10	0.946
6	0.04	0.911	2.08	0.894	0.21	0.842
7	0.04	0.946	2.73	0.921	0.20	0.950
8	0.06	0.996	2.41	1.000	0.27	0.864
9	0.07	0.978	2.37	0.986	0.24	0.890
10	0.21	0.741	0.20	0.971	0.02	0.827
[Dye] ₀ : 100–2000 (μmol/L); solution pH 4; temperature 30°C						
100	0.06	0.994	3.35	0.999	0.43	0.768
250	0.05	0.982	11.00	0.974	1.25	0.896
500	0.05	0.980	13.16	0.963	1.12	0.896
1000	0.05	0.980	13.16	0.963	1.12	0.896
1500	0.05	0.980	13.16	0.963	1.12	0.896
2000	0.05	0.980	13.16	0.963	1.12	0.896
Ionic strength: 0.01–0.05 (mol/L); solution pH 4; [Dye] ₀ : 50 μmol/L; temperature 30°C						
0.01	0.04	0.968	0.60	0.959	0.06	0.991
0.02	0.04	0.962	0.70	0.936	0.07	0.966
0.13	0.05	0.995	0.57	0.985	0.06	0.866
0.05	0.04	0.995	0.56	0.978	0.11	0.837
Temperature: 35–45 (°C); solution pH 4; [Dye] ₀ : 50 μmol/L						
35	0.04	0.994	0.53	0.981	0.09	0.895
40	0.05	0.997	0.89	1.000	0.12	0.848
45	0.04	0.983	1.26	0.963	0.15	0.911

Langmuir model:

$$\text{nonlinear form } q_e = \frac{K_L C_e}{(1 + a_L C_e)}, \quad (16)$$

$$\text{linear form } \frac{C_e}{q_e} = \frac{1}{K_L} + \frac{a_L}{K_L} C_e, \quad (17)$$

where C_e (μmol/L) denotes dye concentration at equilibrium, q_e (μmol/g) represents measure of new coccine adsorbed per unit weight of chitosan 10B at equilibrium, K_F ((μmol/g) (μmol/L)^{-1/n}) and n imply Freundlich isotherm constants showing the aptitude and magnitude of the adsorption. K_T (μmol/L) means Temkin isotherm constant, b (J/mol) relates to the heat of adsorption, R (8.314 (J/mol) K) is an ideal gas constant, T is absolute temperature (K), K_L (L/g) denotes Langmuir constant and a_L (L/μmol) is the Langmuir binding constant. The highest dye adsorption onto chitosan 10B, q_m (μmol/g), was computed from the ratio of K_L/a_L . Table 3 illustrates the values of isotherm and thermodynamic parameters. All adsorption isotherms were matched satisfactorily with Lang-

muir isotherm model preferably than Temkin and Freundlich isotherm models because the highest correlation coefficients ($R^2 \geq 0.991$) were observed in Langmuir model (Table 3). The q_m values were computed to be 90.77 μmol/g at 30°C and 86.67 μmol/g at 45°C, respectively.

Confirmation of Dye Adsorption

FTIR spectrum of chitosan 10B and new coccine loaded-chitosan 10B are exhibited in Fig. 9. The broad band at 3420 cm⁻¹ for the N–H stretching and O–H stretching of chitosan 10B (Fig. 9(1)) was shifted to 3441 cm⁻¹ in dye-loaded chitosan 10B (Fig. 9(2)), which indicates an interaction between the NH/OH group of chitosan 10B and dye molecule [44]. The band at 2878 cm⁻¹ corresponding to C–H stretching in the spectrum of fresh chitosan 10B shifted to 2881 cm⁻¹ after adsorption. The vibration bands at 1649 cm⁻¹ for amide-I (C=O stretching) and at 1599 cm⁻¹ for amide-II (N–H bending) of fresh chitosan 10B (Fig. 9(1))

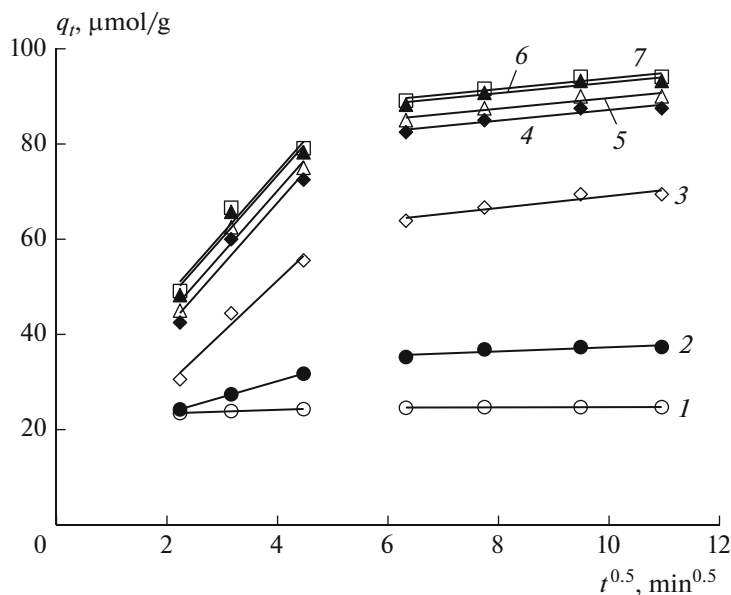


Fig. 7. Characteristic plots of q_t versus $t^{0.5}$ for the new cocaine elimination by chitosan 10B at various initial dye concentration of solutions. Solution pH 4, solution volume—25 mL, adsorbent dosage—0.05 g, temperature—30°C. [New cocaine] $_0$: 1—50, 2—100, 3—250, 4—500, 5—1000, 6—1500, 7—2000 $\mu\text{mol/L}$. The values of k_{id1} ($(\mu\text{mol/g}) \text{min}^{0.5}$) and k_{id2} ($(\mu\text{mol/g}) \text{min}^{0.5}$) are computed in Table 2.

shifted to 1647 and 1595 cm^{-1} in dye-loaded chitosan 10B (Fig. 9(2)). The peak at 1420 cm^{-1} associated with $-\text{CH}_2$ bending in the spectrum of fresh chitosan 10B shifted to 1422 cm^{-1} in dye-loaded chitosan 10B (Fig. 9(2)). The typical bands of polysaccharide backbone appearing at 1153, 1080, 1024 and 897 cm^{-1} of fresh chitosan 10B (Fig. 9(1)) shifted to 1154, 1094, 1022 and 895 cm^{-1} as shown in Fig. 9(2). Hence, the adsorption of new cocaine dye onto chitosan 10B can be confirmed.

Thermodynamics

Thermodynamic research on the adsorption process is essential to inspect the spontaneity of the system. The changes in Gibb's free energy (ΔG kJ/mol), enthalpy (ΔH kJ/mol) and entropy (ΔS (J/mol) K) were computed by using following Eq. [45]:

$$\Delta G = -RT \ln a_L, \quad (18)$$

$$\ln a_L = \frac{\Delta S}{R} - \frac{\Delta H}{RT}, \quad (19)$$

where (a_L l/mol) denotes Langmuir binding constant, R is the universal gas constant (8.314 (J/mol) K) and T is the absolute temperature (K). The slope and y-intercept of the plot $\ln a_L$ versus $1/T$ ($R^2 = 0.950$) were used to calculate the values of ΔH : -94.54 kJ/mol and ΔS : -227.33 (J/mol) K, respectively (Table 3). The negative magnitude of ΔH implies that the new cocaine adsorption onto chitosan 10B pursued exothermic processes. The negative ΔS confirmed the decreased

of randomness due to the strong binding of new cocaine dye with chitosan 10B particles [46]. The value of $|\Delta H|$ is greater than that of $|T\Delta S|$ at all temperatures which signifies that the adsorption process is controlled by enthalpic rather than entropic changes [46]. The Gibb's free energy (ΔG) was calculated to be -24.88 at

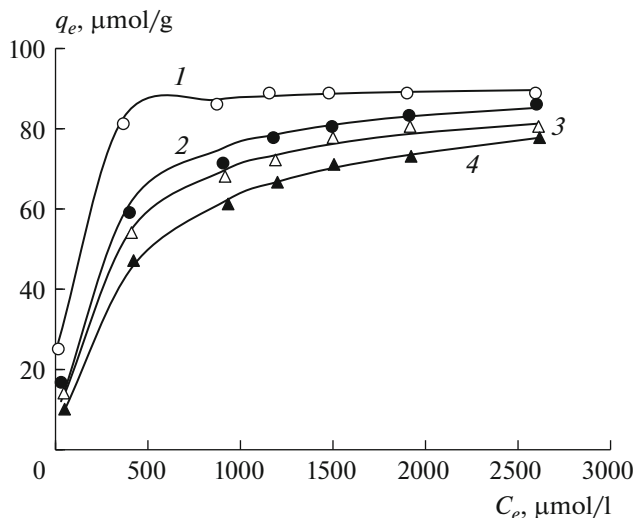


Fig. 8. Adsorption isotherm of new cocaine onto chitosan 10B at different temperatures. Solution pH 4, [New cocaine] $_0$: 50–3000 $\mu\text{mol/L}$, solution volume—25 mL, adsorbent dosage—0.05 g, temperature: 1—30, 2—35, 3—40, 4—45°C. All lines were mimicked by employing Langmuir isotherm Eq. (19), a_L and K_L at numerous temperatures recorded in Table 3.

Table 3. The values of various isotherm constants and thermodynamics for the new coccine adsorption onto chitosan in aqueous media (pH 4)

Isotherm/thermodynamics	Parameters	Temperature, °C			
		30	35	40	45
Freundlich model	$K_F, (\mu\text{mol/g}) (\mu\text{mol/l})^{-1/n}$	28.11	16.22	9.02	7.36
	N	6.41	4.66	3.49	3.28
	R^2	0.971	0.975	0.983	0.969
Temkin model	$K_T, \mu\text{mol/L}$	4.85	0.43	0.12	0.08
	$b, \text{J/mol}$	261.17	213.93	181.17	180.16
	R^2	0.964	0.940	0.952	0.911
Langmuir model	$K_L, \text{L/g}$	1.77	0.47	0.36	0.26
	$a_L, \text{L}/\mu\text{mol}$	19.50×10^{-03}	5.20×10^{-03}	4.10×10^{-03}	3.00×10^{-03}
	$q_m, \mu\text{mol/g}$	90.77	90.38	87.80	86.67
	R^2	0.999	0.991	0.989	0.974
Thermodynamics	$\Delta G, \text{kJ/mol}$	-24.88	-21.89	-21.63	-21.15
	$\Delta H, \text{kJ/mol}$			-94.54	
	$\Delta S, (\text{J/mol}) \text{K}$			-227.33	
	R^2			0.950	

30°C and -21.15 kJ/mol at 45°C, respectively (Table 3). The negative values of ΔG decreased with increasing temperatures which indicates that the adsorption process was spontaneous and favored at low temperatures.

Reuse of the Chitosan 10B

The recyclable adsorbent is very important in industry to assemble an economic wastewater remedy

plant [47]. Figure 10 shows the typical plot of new coccine dye adsorption-desorption-adsorption onto chitosan 10B in aqueous systems. In the adsorption step 1, dye solution (50 $\mu\text{mol/L}$; 25 mL; pH 4) was interacted with chitosan 10B (0.05 g) for 120 min at 30°C whereas the dye release from new coccine-loaded chitosan 10B was measured in 0.1 mol/L NaOH (25 mL; pH 13) for 120 min at 30°C. The value of q_e was measured to be 24.72 $\mu\text{mol/g}$ in the adsorption step 1. In desorption

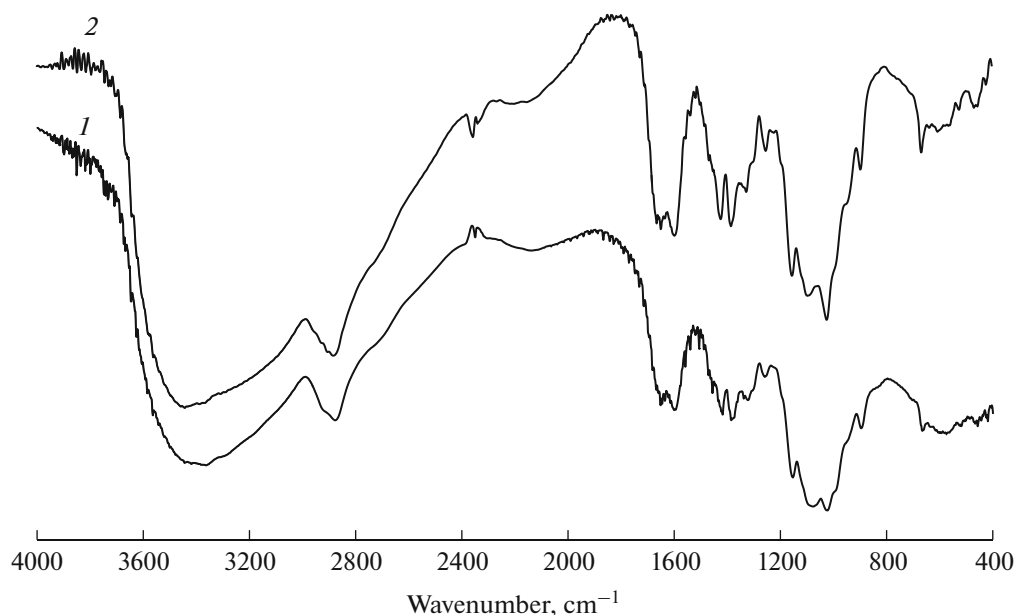


Fig. 9. FTIR spectrum of Chitosan 10B before (1) and after (2) new coccine dye adsorption. The spectra were recorded in KBr.

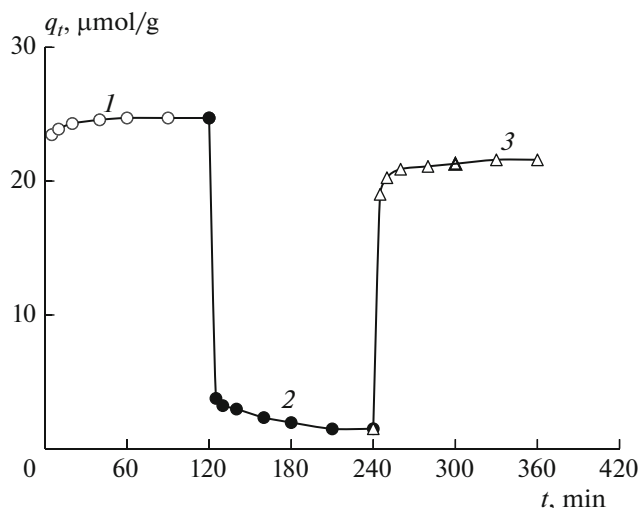


Fig. 10. Adsorption-desorption-adsorption kinetics of new coccine onto chitosan 10B in aqueous medium at 30°C. [New coccine]₀: 50 μmol/L, solution volume—25 mL, adsorbent dosage—0.05 g, 1—adsorption step 1: direct adsorption at pH 4, 2—desorption step—pH 13, 3—adsorption step 2: regenerated chitosan 10B was used at pH 4.

step, new coccine release rate was very fast for primary 20 min and 88% of new coccine was discharged from dye-loaded chitosan 10B in 120 min. It suggests that the anionic new coccine dye molecules was easily liberated from dye loaded-chitosan 10B in strongly basic solution (pH 13). In the adsorption step 2, recycled chitosan 10B was used to adsorb new coccine dye solution (50 μmol/L; 25 mL; pH 4) for 120 min. The quantity of dye adsorption was analogous as noticed in step 1. The value of q_e was found to be 21.59 μmol/g for recycled chitosan 10B. These results indicate that the chitosan 10B can be utilized as an efficient adsorbent for removing new coccine dye from aqueous solution.

CONCLUSIONS

The kinetics, mechanisms, equilibrium and thermodynamics of new coccine dye adsorption onto chitosan 10B were studied in aqueous media. The pH_{pzc} of chitosan 10B was found to be 6.45. The dye adsorption kinetics was inspected in aqueous solution as function of contact time, solution pH, initial dye concentration, ionic strengths and temperatures, respectively. Adsorption capability of the chitosan 10B was raised with increasing of interaction time, dye concentration, and decreased with rising temperatures and ionic strengths, respectively. New coccine elimination by chitosan 10B was maximized at solution pH 4. The pseudo second-order kinetic model fully approves new coccine adsorption kinetics with dynamical behavior. The $q_{e, \text{cal}}$ values computed from pseudo second-order kinetic model are analogous to the $q_{e, \text{exp}}$ values found in batch experiments. In addition, the

observed adsorption kinetic traces are absolutely mimicked traces obtained from numerical analysis based on the pseudo second-order kinetic model and employing the values of k_2 and $q_{e, \text{cal}}$ recorded in Table 1. The Langmuir isotherm model is the best-fit equilibrium isotherm preferably than the Freundlich and the Temkin models for the sorption of new coccine dye onto chitosan 10B. The highest new coccine adsorption capability of chitosan 10B was observed to be 90.77 μmol/g at 30°C. The dye adsorption onto chitosan 10B was proven by FTIR spectroscopy. The values of thermodynamic parameters (ΔH : -94.54 kJ/mol; ΔS : -227.33 (J/mol) K and ΔG : -24.88 kJ/mol at 30°C and -21.15 kJ/mol at 45°C) demonstrated that the new coccine adsorption onto chitosan 10B is spontaneous exothermic physisorption process. The dye-loaded chitosan 10B released new coccine dye in NaOH solution (0.1 mol/L; pH 13) and the recycled chitosan 10B was used in dye adsorption without significant loss its activity. This research confirms that the chitosan 10B can be employed as a productive adsorbent to eliminate new coccine from aqueous solution.

ACKNOWLEDGMENTS

We are thankful to the Ministry of Science and technology, Government of the People's Republic of Bangladesh for giving research grant to Prof. Dr. Tapan Kumar Saha to complete the present work.

REFERENCES

1. Y. M. Kolekar, S. P. Pawar, K. R. Gawai, et al., *Biore-sour. Technol.* **99**, 8999 (2008). <https://doi.org/10.1016/j.biortech.2008.04.073>
2. I. M. Banat, P. Nigam, D. Singh, and R. Marchant, *Biore-sour. Technol.* **58**, 217 (1996). [https://doi.org/10.1016/S0960-8524\(96\)00113-7](https://doi.org/10.1016/S0960-8524(96)00113-7)
3. O. Anjaneya, S. S. Shrishailnath, K. Guruprasad, A. S. Nayak, S. B. Mashetty, and T. B. Karegoudar, *Int. Biodeterior. Biodegrad.* **79**, 64 (2013). <https://doi.org/10.1016/j.ibiod.2013.01.006>
4. T. K. Saha, H. Frauendorf, M. John, S. Dechert, and F. Meyer, *ChemCatChem.* **5**, 796 (2013). <https://doi.org/10.1002/cctc.201200475>
5. T. K. Saha, S. Karmaker, S. Debnath, and M. I. A. Biswas, *Russ. J. Phys. Chem. A* **94**, 2723 (2020). <https://doi.org/10.1134/S0036024420130233>
6. A. A. Kashmeri, F. Nawaz, M. Yousal, A. Shameem, M. Sh. Mahr, J. Iqbal, M. Shafique, and M. A. Javed, *Russ. J. Phys. Chem. B* **14**, 552 (2020). <https://doi.org/10.1134/S1990793120030069>
7. E. M. Bayan, T. G. Lupeiko, and L. E. Pustovaya, *Russ. J. Phys. Chem. B* **12**, 923 (2018). <https://doi.org/10.1134/S1990793118050159>
8. F. Mcyotto, Q. Wei, D. K. Macharia, M. Huang, C. Shen, and C. W. K. Chow, *Chem. Eng. J.* **405**, 126674 (2021). <https://doi.org/10.1016/j.cej.2020.126674>

9. K. Guo, B. Gao, R. Li, W. Wang, Q. Yue, and Y. Wang, *Environ. Sci. Pollut. Res.* **25**, 2083 (2018).
<https://doi.org/10.1007/s11356-017-0835-z>
10. C. Zhijiang, X. Ping, Z. Cong, Z. Tingting, G. Jie, and Z. Kongyin, *Cellulose* **25**, 5123 (2018).
<https://doi.org/10.1007/s10570-018-1914-0>
11. S. Karmaker, A. J. Nag, and T. K. Saha, *Cellulose Chem. Technol.* **53**, 373 (2019).
<https://doi.org/10.35812/CelluloseChemTechnol.2019.53.38>
12. S. Karmaker, A. J. Nag, and T. K. Saha, *Russ. J. Phys. Chem. A* **94**, 2349 (2020).
<https://doi.org/10.1134/S0036024420110126>
13. T. K. Saha, S. Karmaker, H. Ichikawa, and Y. Fukumori, *J. Colloid Interface Sci.* **286**, 433 (2005).
<https://doi.org/10.1016/j.jcis.2005.01.037>
14. V. B. Ivanov, A. A. Zavodchikova, I. I. Barashkova, E. V. Solina, and A. M. Wasserman, *Russ. J. Phys. Chem. B* **8**, 233 (2014).
<https://doi.org/10.1134/S1990793114020067>
15. M. Khadhraoui, H. Trabelsi, M. Ksibi, S. Bouguerra, and B. Elleuch, *J. Hazard. Mater.* **161**, 974 (2009).
<https://doi.org/10.1016/j.jhazmat.2008.04.060>
16. P. Pandit and S. Basu, *J. Colloid Interface Sci.* **245**, 208 (2002).
<https://doi.org/10.1006/jcis.2001.7939>
17. R. R. M. Khan, A. Adnan, M. Pervaiz, M. A. Raza, and M. Y. Naz, *Russ. J. Phys. Chem. B* **10**, 517 (2016).
<https://doi.org/10.1134/S1990793116030234>
18. K. N. Aboua, Y. A. Yobouet, K. B. Yao, D. L. Goné, and A. Trokourey, *J. Environ. Manage.* **156**, 10 (2015).
<https://doi.org/10.1016/j.jenvman.2015.03.006>
19. Y. Li, Q. Du, T. Liu, et al., *Chem. Eng. Res. Des.* **91**, 361 (2013).
<https://doi.org/10.1016/j.cherd.2012.07.007>
20. E. Errais, J. Duplay, M. Elhabiri, et al., *Colloids Surf., A* **403**, 69 (2012).
<https://doi.org/10.1016/j.colsurfa.2012.03.057>
21. G. McKay, *Chem. Eng. Sci.* **39**, 129 (1984).
[https://doi.org/10.1016/0009-2509\(84\)80138-4](https://doi.org/10.1016/0009-2509(84)80138-4)
22. J. X. Lin, S. L. Zhan, M. H. Fang, X. Q. Qian, and H. Yang, *J. Environ. Manage.* **87**, 193 (2008).
<https://doi.org/10.1016/j.jenvman.2007.01.001>
23. Y. S. Ho and G. McKay, *Chem. Eng. J.* **70**, 115 (1998).
[https://doi.org/10.1016/S0923-0467\(98\)00076-1](https://doi.org/10.1016/S0923-0467(98)00076-1)
24. X. Ren, X. Zhang, L. Zhang, and R. Han, *Desalin. Water Treatm.* **51**, 4514 (2013).
<https://doi.org/10.1080/19443994.2012.741776>
25. T. K. Saha, R. K. Bishwas, S. Karmaker, and Z. Islam, *ACS Omega* **5**, 13358 (2020).
<https://doi.org/10.1021/acsomega.0c01493>
26. S. Karmaker, M. N. Uddin, H. Ichikawa, Y. Fukumori, and T. K. Saha, *J. Environ. Chem. Eng.* **3**, 583 (2015).
<https://doi.org/10.1016/j.jece.2014.09.010>
27. S. Karmaker, T. Sen, and T. K. Saha, *Polym. Bull.* **72**, 1879 (2015).
<https://doi.org/10.1007/s00289-015-1378-4>
28. S. Karmaker, F. Sintaha, and T. K. Saha, *Adv. Biol. Chem.* **9**, 1 (2019).
<https://doi.org/10.4236/abc.2019.91001>
29. M. Kosmulski, *J. Colloid Interface Sci.* **337**, 439 (2009).
<https://doi.org/10.1016/j.jcis.2009.04.072>
30. M. M. Rahman, N. Akter, M. R. Karim, et al., *J. Environ. Chem. Eng.* **2**, 76 (2014).
<https://doi.org/10.1016/j.jece.2013.11.023>
31. L. Ai, C. Zhang, F. Liao, Y. Wang, K. Li, L. Meng, and J. Jiang, *J. Hazard. Mater.* **198**, 282 (2011).
<https://doi.org/10.1016/j.jhazmat.2011.10.041>
32. P. Udaybhaskar, L. Iyengar, and A. V. S. P. Rao, *J. Appl. Polym. Sci.* **39**, 739 (1990).
<https://doi.org/10.1002/app.1990.070390322>
33. B. K. Nandi, A. Goswami, and M. K. Purkait, *J. Hazard. Mater.* **161**, 387 (2009).
<https://doi.org/10.1016/j.jhazmat.2008.03.110>
34. S. M. O. Brito, H. M. C. Andrade, L. F. Soares, and R. P. Azevedo, *J. Hazard. Mater.* **174**, 84 (2010).
<https://doi.org/10.1016/j.jhazmat.2009.09.020>
35. S. Lagergren, *K. Sven. Vetenskapsakad. Handl.* **24**, 1 (1898).
36. Y. S. Ho and G. McKay, *Process Biochem.* **34**, 451 (1999).
[https://doi.org/10.1016/S0032-9592\(98\)00112-5](https://doi.org/10.1016/S0032-9592(98)00112-5)
37. S. Y. Elovich and O. G. Larinov, *Izv. Akad. Nauk SSSR, Otd. Khim. Nauk.* **2**, 209 (1962).
38. T. K. Saha, N. C. Bhoumik, S. Karmaker, M. G. Ahmed, H. Ichikawa, and Y. Fukumori, *Clean-Soil, Air, Water* **39**, 984 (2011).
<https://doi.org/10.1002/clen.201000315>
39. W. J. Weber and J. C. Morris, *J. Sanit. Eng. Div. Proc. Am. Soc. Civ. Eng.* **89**, 31 (1963).
<https://doi.org/10.1061/JSEDAI.0000430>
40. A. Abdelhay, A. A. Bsoul, A. Al-Othman, N. M. Al-Ananzeh, I. Jum'h, and A. A. Al-Taani, *Adsorp. Sci. Technol.* **36**, 46 (2018).
<https://doi.org/10.1177%2F0263617416684347>
41. H. Freundlich, *Z. Phys. Chem.* **57**, 384 (1906).
<https://doi.org/10.1515/zpch-1907-5723>
42. M. I. Temkin and V. Pyzhev, *Acta Physicochim. USSR* **12**, 327 (1940).
43. I. Langmuir, *J. Am. Chem. Soc.* **40**, 1361 (1918).
<https://doi.org/10.1021/ja02242a004>
44. S. Pervin, C. K. Saha, S. Karmaker, and T. K. Saha, *Polym. Bull.* **78**, 4527 (2021).
<https://doi.org/10.1007/s00289-020-03331-z>
45. Y. Liu, *Colloids Surf., A* **274**, 34 (2006).
<https://doi.org/10.1016/j.colsurfa.2005.08.029>
46. A. A. Atia, A. M. Donia, and W. A. Al-Amrani, *Chem. Eng. J.* **150**, 55 (2009).
<https://doi.org/10.1016/j.jece.2008.12.004>
47. B. Zhao, W. Xiao, Y. Shang, H. Zhu, and R. Han, *Arab. J. Chem.* **10**, S3595 (2017).
<https://doi.org/10.1016/j.arabjc.2014.03.010>